Simulation of four-wheeled robot chassis taking into account contact interaction

A.Y. Chekin[1], A.V. Kukovinets[2]

[1]Federal State Unitary Enterprise “State Research Institute of Aviation Systems”, Viktorenko Street 7, Moscow, Russia, 125319
[2]MIREA – Russian Technological University, Prospekt Vernadskogo 78, Moscow, Russia, 119454

Abstract. One of the tasks of the development and research of moving objects is the modeling of the controlled object. To solve the control synthesis problem, the development of models of mobile ground-based robots is a well-developed area. However, there are situations when the movement of the developed model does not correspond to the experimental data due to the fact that complex processes of contact interaction between the robot chassis and the surface of the ground or the object along which the robot moves are not taken into account. Because of this, errors may occur in the control loops. The paper proposes a robot movement simulation based on a model-based design method. The chassis has a four-wheeled architecture. All wheels interact with the ground through contact interaction and create forces and torques. The obtained results allow us to develop more complete motion models of ground-based robots.

1. Introduction

Dynamic vehicle models are important tools for research and development both in the automotive industry and in the development of autonomous robotic vehicles that perform peaceful and military tasks. The development of the chassis is one of the fundamental stages of the construction of robotic vehicles that move on complex surfaces under the influence of gravity both from Earth and from other object in the Universe. The correlation of data obtained in the course of modeling and in the course of full-scale experiment largely depends on the completeness of the description of the mathematical model and taking into account the impact of forces that affect the movement of the physical model.

This paper considers the simulation of the movement of a robot consisting of a base with four supports of chassis. Each support is a spring-loaded shock absorber with rotating round wheels. To control the movement of the robot, both the wheels and the turn of the chassis supports are supplied with a control torques from motors.

In the proposed model, the base has six degrees of freedom (DOF), the support has two DOF: one degree of rotation around the vertical axis and one degree of movement along the vertical axis relative the body axes, the wheel has one degree of rotation around the axis in the horizontal plane.

The robot is affected by gravitational forces and contact forces. Aerodynamic forces are not taken into account due to the low speeds of the object relative to the air.

2. Models of chassis elements

2.1. Support

In order to describe the correct and complete movement of a moving body, it is necessary to take into account the fact that no one struts can be absolutely rigid. Therefore, the four-wheeled robot chassis model includes two elastic joints of the body and wheels. Each struts makes a significant contribution to the movement of the robot base relative to the movement surface on which the robot moves. The general view of the strut is shown in figure 1 [1].

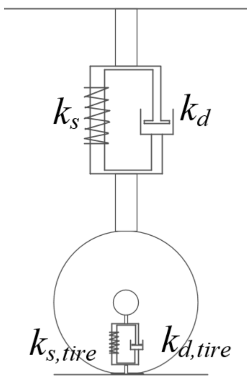

Figure 1. General view of the strut.

Here k_s – stiffness coefficient of the support spring, k_d – damping coefficient of the support shock absorber.

As a support part, can be used a pneumatic wheel, or any material from which the wheel is made of – plastic, rubber or metal, which has elastic properties and is described by the stiffness coefficient of the wheel spring $k_{s,tire}$ and the damping coefficient of the wheel $k_{d,tire}$.

2.2. Suspension

In this paper, the front supports are rotational, the rear are fixed. With the rotation of the steered wheels at α_{left} and α_{right} angles appear longitudinal and lateral forces action on the base figure 2 [2]:

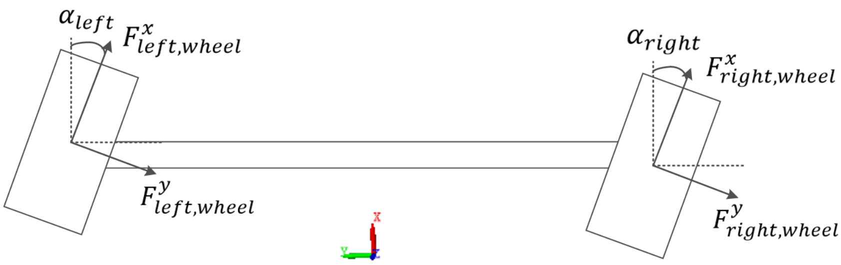

Figure 2. Turning the steered wheels – yaw motion of the robot.

$$F^x_{wheels} = F^x_{left,wheel}\cos(\alpha_{left}) - F^y_{left,wheel}\sin(\alpha_{left}) + \\ + F^x_{right,wheel}\cos(\alpha_{right}) - F^y_{right,wheel}\sin(\alpha_{right}) \tag{1}$$

$$F^{y}_{wheels} = F^{y}_{left,wheel}\cos(\alpha_{left}) + F^{x}_{left,wheel}\sin(\alpha_{left}) + \\ + F^{y}_{right,wheel}\cos(\alpha_{right}) + F^{x}_{right,wheel}\sin(\alpha_{right}) \tag{2}$$

Figure 3 shows the action of the elastic forces from the left and right springs $F^z_{s,left}$ and $F^z_{s,right}$, as well as the forces of the dampers $F^z_{d,left}$ and $F^z_{d,right}$ [3], [4]. O – the center of the roll. The distance between the elastic elements is l.

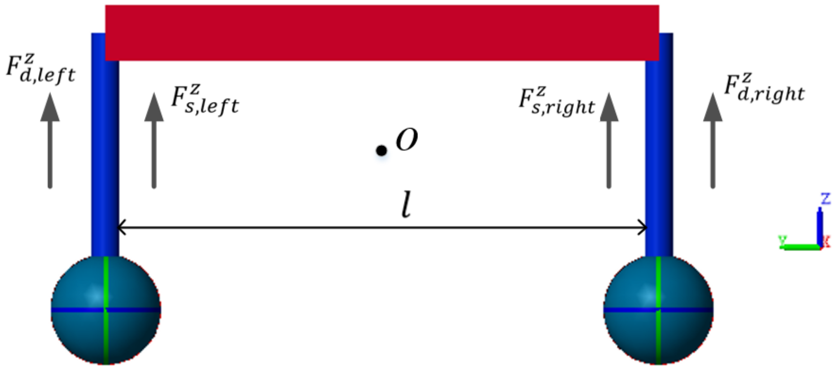

Figure 3. Determine the roll torque caused by spring and damper.

The torque:

$$M^x_{roll} = F^z_{s,left}\frac{l}{2} - F^z_{s,right}\frac{l}{2} + F^z_{d,left}\frac{l}{2} - F^z_{d,right}\frac{l}{2} \tag{3}$$

Equations describing an ideal mechanical linear spring [5]:

$$F_s = k_s x \tag{4}$$

$$x = x_0 + x_R - x_C \tag{5}$$

$$v = \frac{dx}{dt} \tag{6}$$

where F_s – force transmitted through the spring; k_s – spring rate; x – relative displacement (spring deformation); x_0 – spring initial displacement (initial deformation), the spring can be initially compressed ($x_0 > 0$) or stretched ($x_0 < 0$); x_R,x_C – absolute displacements of terminals R and C, respectively; v – relative velocity; t – time.

Equations, describing an ideal mechanical translational viscous damper [6]:

$$F_d = k_d v \tag{7}$$

$$v = v_R - v_C \tag{8}$$

where F_d – force transmitted through the damper; k_d – damping (viscous friction) coefficient; v – relative velocity; v_R, v_C – absolute velocities of terminals R and C, respectively. k_s and k_d – coefficients set in process of development of the robot chassis model.

3. Contact interaction

When a mobile robot moves on a surface, the forces shown in figure 4 in the xOz plane act on its suspension. The normal reaction force N and the friction force F_{fric} act directly at the point of contact between the wheel and the surface. In general, the wheels are affected by the driving torque from motors. The total gravity $F_{mg} = mg$ is applied to the center of mass of the considered subsystem. The projection F_{mg} to the vertical axis z depends on the inclination angle β.

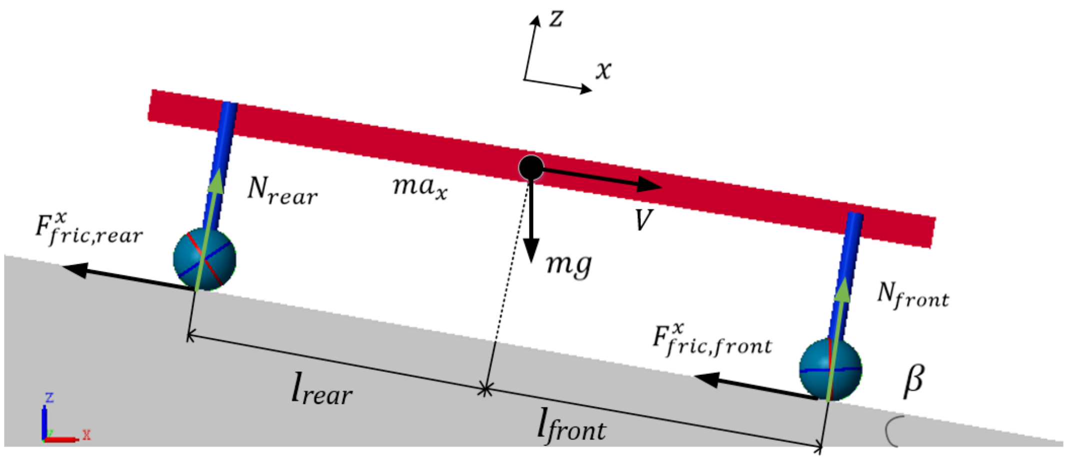

Figure 4. Forces acting to the robot's suspension.

Expressions for calculating longitudinal, lateral and vertical forces are:

$$F^x = -F^x_{fric,rear,left} - F^x_{fric,rear,right} - F^x_{fric,front,left} - F^x_{fric,front,right} + F_{mg}\sin\beta \quad (9)$$

F^y is defined similarly to F^x.

$$F^z = N_{rear,left} + N_{rear,right} + N_{front,left} + N_{front,right} - F_{mg}\cos\beta \quad (10)$$

Expressions for calculating the torques of the corresponding forces are determined from the figures 5, 6.

$$\begin{aligned} M^x = N_{rear,left}l_1 - N_{rear,right}l_1 + N_{front,left}l_1 - N_{front,right}l_1 + \\ + F^y_{fric,rear,left}l_{sup} + F^y_{fric,front,left}l_{sup} + \\ + F^y_{fric,rear,right}l_{sup} + F^y_{fric,front,right}l_{sup} \end{aligned} \quad (11)$$

M^y is defined similarly to M^x.

In figure 5 l_{sup} – the length of the support, l_1 – half the distance between the wheels.

$$\begin{aligned} M^z = F^y_{fric,front,left}l_{front} - F^x_{fric,front,left}l_1 + F^y_{fric,front,right}l_{front} + \\ + F^x_{fric,front,right}l_1 - F^y_{fric,rear,left}l_{rear} - F^x_{fric,rear,left}l_1 - \\ - F^y_{fric,rear,right}l_{rear} + F^x_{fric,rear,right}l_1 \end{aligned} \quad (12)$$

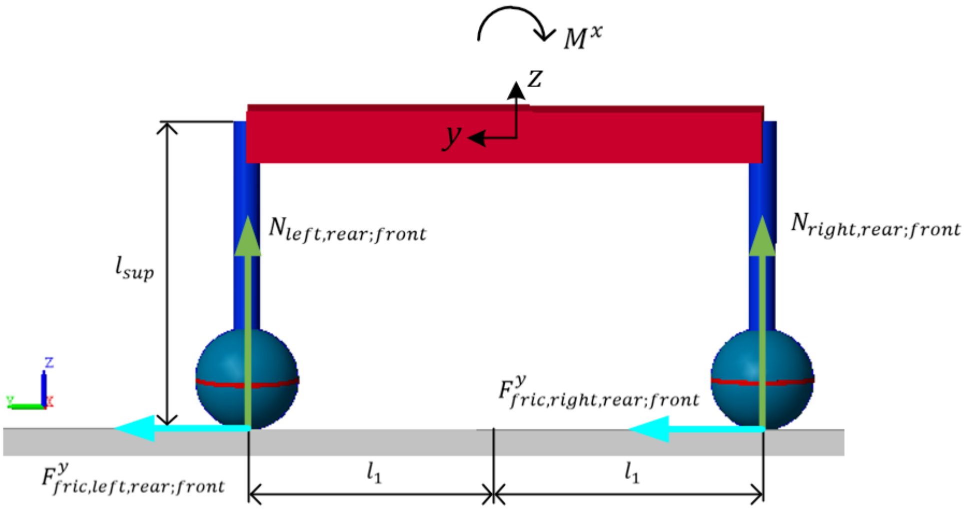

Figure 5. Determining the torque M^x.

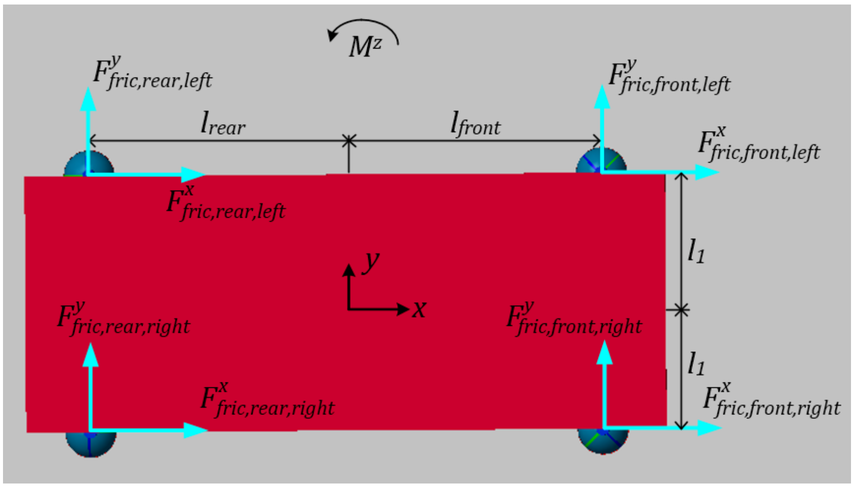

Figure 6. Determining the torque M^z.

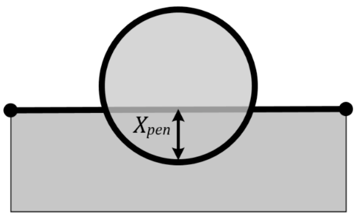

Figure 7. Penetration.

3.1. Contact force laws [7]

A linear spring-damper resists penetration. Damping force is 0 as penetration decreases. Force is applied only along the direction of penetration (figure 7). Linear circle to line law:

$$F_x = \begin{cases} k_{s,tire} \cdot x_{pen} + k_{d,tire} \cdot v_{pen} & \text{if } x_{pen} > 0, v_{pen} > 0 \\ k_{s,tire} \cdot x_{pen} & \text{if } x_{pen} > 0, v_{pen} < 0 \\ 0 & \text{if } x_{pen} \leqslant 0 \end{cases} \quad (13)$$

Nonlinear circle to line law is the same as linear except:

(i) Stiffness force increases exponentially with penetration: $k_{s,tire} \cdot (x_{pen})^e$, where e is parameter penetration component;

(ii) Damping force increases gradually during initial penetration: $k_{d,tire} \cdot v_{pen} \cdot SmoothStep$, where $SmoothStep$ is a polynomial whose value increases from 0 to 1 as the penetration increases from 0 to parameter penetration for full damping.

3.2. Friction forces law [8]

Friction force is product of coefficient of friction μ and normal force N:

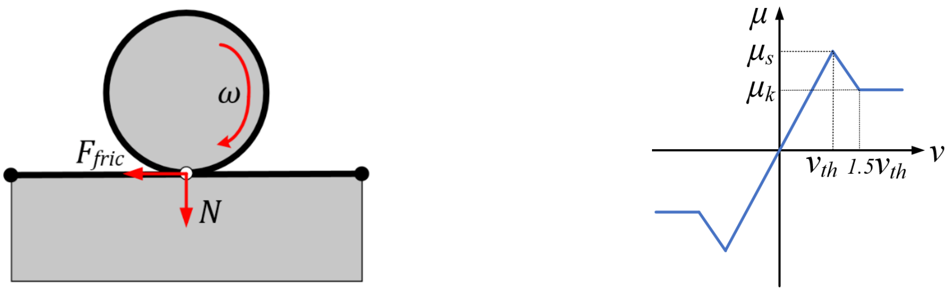

Figure 8. Friction force and coefficient.

$$F_{fric} = \mu N \quad (14)$$

where the coefficient of friction is a function of the relative velocity at the point of contact.

$$\mu = \begin{cases} v_{poc} \cdot \dfrac{\mu_s}{v_{th}} & \text{if } v_{poc} < v_{th} \\ \mu_s - v_{poc} \cdot \dfrac{\mu_s - \mu_k}{0.5v_{th}} & \text{if } v_{th} \leqslant v_{poc} \leqslant 1.5v_{th} \\ \mu_k & \text{if } v_{poc} > v_{th} \end{cases} \quad (15)$$

where v_{poc} – velocity at point of contact; v_{th} - threshold velocity.

In figure 8b, μ_s – static friction coefficient; μ_k – kinematic friction coefficient; v_{th} – velocity threshold.

4. Complete model

To obtain a complete mathematical model of an object, it is necessary to take into account its translational and rotational motion. In this paper, it is assumed that at low speeds of the robot movement, the aerodynamic force, the influence of which is considered in [9], [10], and the Archimedean force have a slight influence to the dynamic of the system, therefore these forces are excluded from consideration. General equations of object dynamics are given in [11].

The dynamic equations of the translational motion in vector form:

$$m\frac{\mathrm{d}\vec{V}}{\mathrm{d}t} + \vec{\omega} \times \vec{V} = \sum \vec{F} \quad (16)$$

The equations of angular motion dynamics that determine the change of the torque vector of the amount of motion K can be written relative to coupled coordinate system $Oxyz$ in the following form:

$$\frac{\mathrm{d}\vec{K}}{\mathrm{d}t} + \vec{\omega} \times \vec{K} = \sum \vec{M} \quad (17)$$

For the model under consideration, the right side of equation 16 is formed from the equations 1 – 12, 4 – 10, 13 – 15. And the right side of the equation 17 – from the equations 3 – 6, 11, 12, 14, 15. The mathematical model is rather complex, and the numerical solution of such system of equations is very laborious and consuming. A mistake or inaccuracy in describing at least one force or torque leads to incorrect solutions of the total movement due to the mutual cross-influence of the movements. An efficient and flexible calculation of the proposed four-wheeled robot chassis model is possible using the model-based design method in MATLAB/Simulink. In this development environment, all impacts and contact interactions are automatically accounted by using the Contact Forces Library. The proposed approach allows to conveniently and quickly configure and explore the parameters of the model, add new interactions and repeatedly reproduce the experiments. The complete model of the robot base with a chassis and a flat ground surface developed in Simulink is shown in figure 9. Submodels of spring-loaded shock absorbers are located in the «Spring. . . » blocks. The contact interaction submodels are located in the «Contact. . . » blocks.

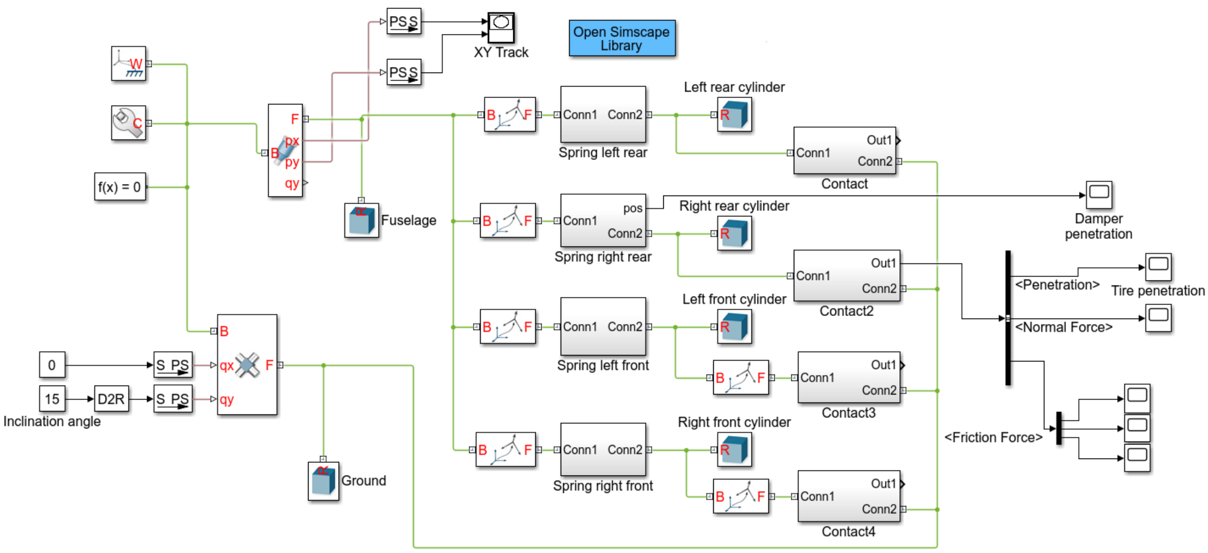

Figure 9. Complete model in Simulink.

Figure 10 shows the object in three-dimensional space.

5. Simulation results

The simulation was performed for the following model parameters: $k_{s,rear} = 5000N/m$; $k_{d,rear} = 500N/(m/s)$; $k_{s,front} = 10^4N/m$; $k_{d,front} = 1000N/(m/s)$; $k_{s,tire} = 10^5N/m$; $k_{d,tire} = 10^4N/(m/s)$; $m = 339kg$; $\mu_s = 0.8$; $\mu_k = 0.5$; $v_{th} = 0.001m/s$.

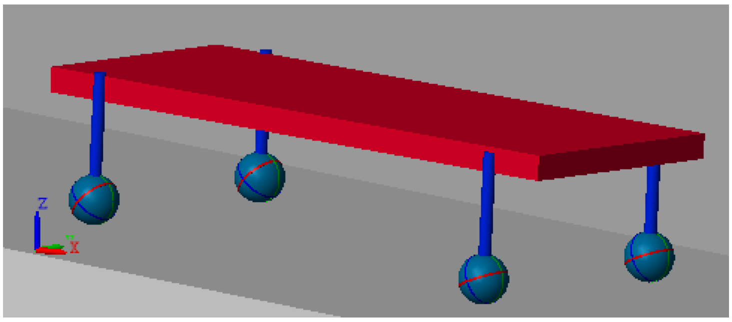

Figure 10. Model in three-dimensional space.

During initialization for clarity of the transient process the robot falls from a height of $h = 2.4m$ to a surface with an angle of inclination $\beta = 15°$. The length of robot base is $5m$, width is $2m$, height is $0.2m$, the supports are $1m$ long and their radius is $0.05m$, the radius of the wheels is $0.2m$. The front supports are rotated at 45 degrees to simulate rotation and do an exploration of forces of friction on an inclined plane.

Chosen nonlinear force law with parameters: penetration for full damping is $10^{-4}m$, penetration exponent is 1.

Solver: $ode23t$ with variable-step, where max step size is $1e$-3, relative tolerance is $1e$-7 and absolute tolerance is $1e$-6.

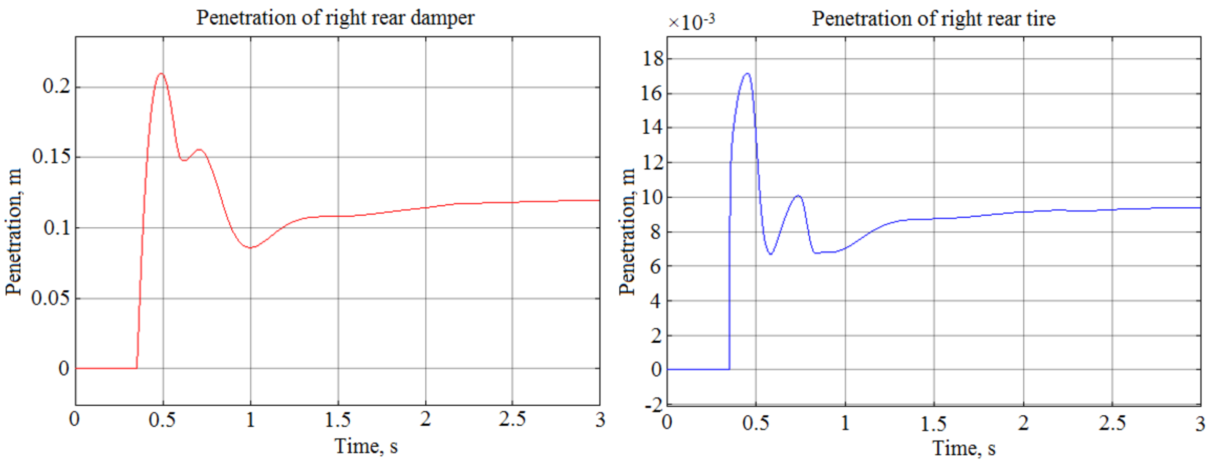

Figure 11. Penetrations of damper and tire.

Figure 11 shows the penetrations of the rear right damper and tire corresponding to the figure 1 while robot falls to a plane and then moves on it during 3 seconds. The transient process comes to a steady state, because after landing of robot the deformation of the shock absorber has approximately a constant value due to the flatness of the surface.

Figure 12 shows the projections of the friction force on the x- and y-axis acting on the rear right tire. The type of the obtained graphs is determined by taking into account the initial rotation of the front supports of the model.

Figure 13 shows normal force acting to the rear right tire. The graph is given after the moment of landing.

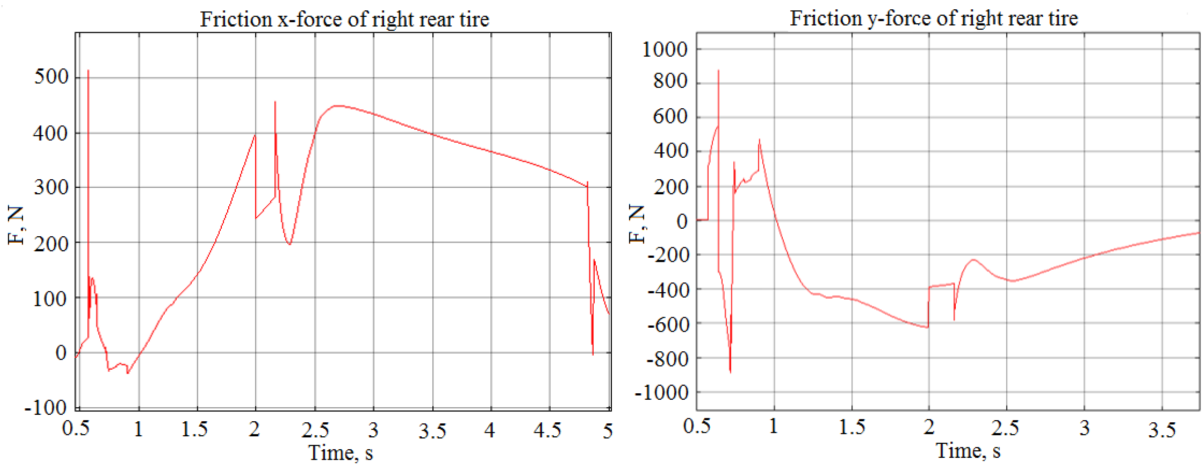

Figure 12. Friction x- and y-forces.

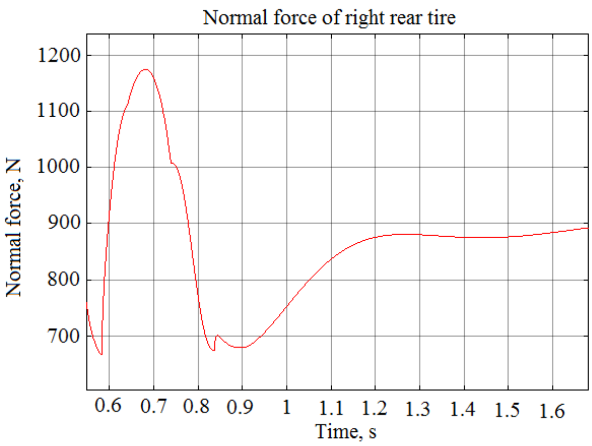

Figure 13. Normal force.

Figure 14 shows the trajectory of the centre of mass of the robot moving under the influence of gravity on an inclined plane. The robot's rear wheels supports are fixed at a zero angle position and the front wheels supports are fixed at a 45 degrees position. The unsteadiness of the movement is caused by taking into account the forces of contact interaction, in particular the nonlinear and non-stationary dependence of the friction forces of the wheels and the contact surface.

6. Conclusion

The capabilities of model-based design allow to perform physical modeling of the developed object taking into account all the necessary parameters, as well as to conduct numerical integration when calculating the contact interaction of the physical model of a mobile object with the surface on which it should move. Often there are situations when the experimental movement of the ground-based robot does not correspond to the movement of its theoretical model. To avoid such situations, it is expediently to synthesize a more complete physical model using model-based design.

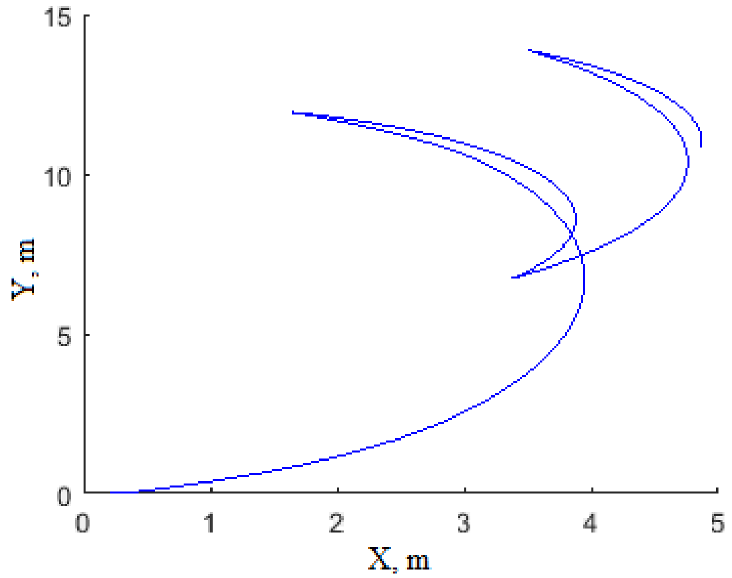

Figure 14. Track of robot's center of mass.

7. References

[1] Jazar, R. Vehicle dynamics: theory and application – New York: Springer-Verlag, 2008. – 1022 p.
[2] Sedran, S. A truck dynamics model for driving simulators. Sweden: Department of Applied Mechanics – Chalmers University of Technology, 2016. – 99 p.
[3] Patil, V. Generic and complete vehicle dynamic models for open-source platforms // Mechanical, Maritime and Materials Engineering Department – Netherlands, 2017. – 112 p.
[4] Bruzelius, F. A Basic Vehicle Dynamics Model for Driving Simulators / F. Bruzelius, J. Gomez Fernandez, B. Augusto // International Journal of Vehicle Systems Modelling and Testing. – 2013. – Vol. 8(4). – P. 364-386.
[5] Rill, G. Vehicle dynamics – Brasil: Hochschule Regensburg University of Applied Sciences, 2007. – 200 p.
[6] MathWorks. Translational Damper [Electronic resource]. – Access mode: https://www.mathworks.com/help/physmod/sdl/ref/translationaldamper.html?searchHighlight=damper&stid=docsrchtitle (25.12.2019).
[7] MathWorks. Contact Force Laws [Electronic resource]. – Access mode: https://www.mathworks.com/matlabcentral/mlc-downloads/downloads/submissions/64001/versions/5/previews/Libraries/ContactLib/Libraries/Help/html/ForceLaws.html (25.12.2019).
[8] MathWorks. Friction Force Laws [Electronic resource]. – Access mode: https://www.mathworks.com/matlabcentral/mlc-downloads/downloads/submissions/65316/versions/6/previews/Libraries/CFL Libs/Libraries/Help/html/FrictionLaws.html (25.12.2019).
[9] Glaser, S. Lateral wind force and torque estimation for a driving assistance / S. Glaser, S. Mammar, D. Dakhlallah // 17th IFAC World Congress, 2008. – P. 5688-5693.
[10] Haggag, S. Aerodynamic Forces Impact on Vehicle Braking Longitudinal Dynamics with a Sliding Mode Controller / S. Haggag, A. Mansouri // SAE Technical Paper. – 2016. – Vol. 01-0460. DOI: 10.4271/2016-01-0460.
[11] Bushgens, G.S. Aerodynamics, stability and controllability of supersonic aircraft – M.: Nauka. Fizmatlit, 1998. – 816 p.